Thickness-dependent magnetization reversal behavior of lithographic IrMn/Fe ring structures

Yu-feng Hou and Kannan M. Krishnan

Citation: J. Appl. Phys. **111**, 07B905 (2012); doi: 10.1063/1.3672827
View online: http://dx.doi.org/10.1063/1.3672827
View Table of Contents: http://jap.aip.org/resource/1/JAPIAU/v111/i7
Published by the American Institute of Physics.

Thickness-dependent magnetization reversal behavior of lithographic IrMn/Fe ring structures

Yu-feng Hou and Kannan M. Krishnan[a)]
Department of Materials Science, University of Washington, Seattle, Washington 98195, USA

(Presented 2 November 2011; received 23 September 2011; accepted 26 October 2011; published online 1 March 2012)

We systematically studied the effect of exchange bias (EB) on the magnetization reversal behavior in lithographic IrMn/Fe rings and their unbiased Fe counterparts, with the thickness of the Fe layer, t_{Fe}, varying from 10 to 80 nm. For unbiased and exchange biased rings, an evolution in the shape of the hysteresis loop from single-step to double-step is observed as t_{Fe} increases. However, for EB rings, this transition happens at larger thickness, which is attributed to the uniaxial anisotropy induced by exchange bias in the Fe layer. The strength of the magnetic anisotropy induced by exchange bias is investigated by fitting the angular dependence of the exchange bias field H_{eb} at different Fe thickness. © *2012 American Institute of Physics*. [doi:10.1063/1.3672827]

INTRODUCTION

With the advancement in fabrication techniques to miniaturize the physical dimensions of magnetic elements, there has been extensive research in lithographically defined structures from both application and scientific points of view.[1] Of particular interest is the magnetization reversal in thin film ring structures due to their highly reproducible switching behavior and distinct magnetic states,[2,3] namely the flux-closure or "vortex" state, in which the magnetization is oriented circumferentially without any domain walls,[4] and the "onion" state with two opposite head-on domain walls.[5] Ring elements have thus been proposed as a potential candidate for magnetic random access memories[6] and magnetic biosensors[7]. In order to control the magnetic states and the switching process of ring structures, techniques such as fabricating notches in the ring,[8] decentering the ring core[9] and creating artificial defects in the ring by a focus ion beam[10] have been used.

As a tunable source of unidirectional anisotropy, exchange bias (EB) can be introduced to thin-film ring structures by employing a ferromagnetic (FM)/antiferromagnetic (AFM) bilayer structure.[11] However, so far, reported work on EB rings is very limited.[12–15] Exchange bias induced asymmetric magnetization behavior along the bias direction has been observed in magnetic ring structures,[16] but the detailed mechanism of magnetic reversal is not well understood.

In this paper, micron-size EB IrMn/Fe ring structures with systematic thickness variation of the Fe layer were fabricated and the evolution of their magnetization reversal mechanism was studied using magneto-optical Kerr effect (MOKE) magnetometry. We observed that the magnetization reversal in ring structures is significantly modified due to EB. The evolution in EB field, H_{eb}, is also investigated as a function of the Fe layer thickness.

IrMn/Fe exchange biased ring arrays with the thickness for IrMn, t_{IrMn}, fixed at 10 nm and for Fe, t_{Fe}, varying from 10 to 80 nm, were patterned on thermally oxidized Si substrates via a mask-transfer lithographic process.[17] First, 1 μm thick polymer resist ring arrays were fabricated on the substrate by photolithography. Then, a 170 nm thick Mo sacrificial layer was deposited onto the resist ring patterns in an ion beam sputtering system, with a base pressure of 1×10^{-8} Torr and followed by ultrasonic assisted chemical lift-off of the resist rings. This step created Mo anti-ring patterns on the substrate. Finally, multilayers with structure Ta (1 nm)/Cu (5 nm)/IrMn (10 nm)/ Fe (t_{Fe} nm)/Ta (3 nm) were sputtered onto the Mo anti-ring pattern obtained in the previous step, and then Mo was etched away by H_2O_2 solution, leaving only multilayer ring arrays on the substrate; the structure of the exchange biased rings is shown in Fig. 1(a). The two bottom layers, Ta (1 nm)/Cu (5 nm), were employed as seed layers to favor [111] texture of IrMn.[18] A 3 nm Ta capping layer was deposited on the top to protect the whole structure from oxidation. In order to introduce an EB, the as-prepared sample was heated to 600 K in vacuum and then cooled to room temperature under an external field of 200 Oe applied in the sample surface plane. To facilitate the understanding of the effect of EB, another set of reference samples without the antiferromagnetic layer, i.e., Ta (1 nm)/Cu (5 nm)/Fe (t_{Fe} nm)/Ta (3 nm), were also prepared in the same process, as shown in Fig. 1(b). Figure 1(c) shows scanning electron microscope images of the multilayer ring arrays and a detailed view of a single ring. Both the exchange biased and unbiased rings showed a circular shape with outer/inner diameter d_{out}/d_{in}=2.4 μm/ 0.8 μm, and inter-ring distance of 3 μm, which was large enough to ensure the dipolar interaction between the rings were negligible.

M-H hysteresis loops of both exchange biased and unbiased ring samples were subsequently measured at room temperature using a magneto-optical Kerr effect (MOKE) setup with external field applied in a longitudinal geometry. To improve the signal-to-noise ratio, each loop was obtained by averaging the measured results over 20 times. Hysteresis loops of the 10 nm [Fig. 2(a)], 30 nm [Fig. 2(b)], and 50 nm [Fig. 2(c)] unbiased ring samples were chosen to show the complete evolution of the hysteresis behavior with thickness in unbiased Fe rings. The red and blue curves in the figure respectively represent the descending and

[a)]Author to whom correspondence should be addressed. Electronic mail: kannanmk@uw.edu.

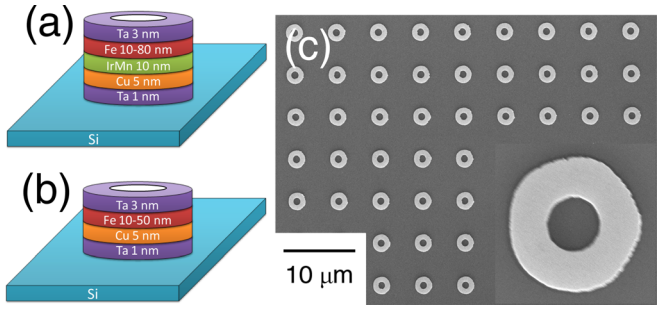

FIG. 1. (Color online) (a) Schematic structure of the multilayer EB IrMn/Fe ring arrays. (b) Schematic structure of the multilayer unbiased Fe ring arrays. (c) Scanning electron microscopic images of the sample. A detailed image of one ring is shown on the bottom right corner.

ascending branches of the loop. The first order derivative, dM/dH, of the descending branch is plotted in the inset at the right bottom corner of each figure. The 10 nm unbiased ring shows a single step transition from positive saturation to negative saturation, at the measured coercivity of $H_c = -75$ Oe [Fig. 2(a)]. The distribution of the switching field, presented by the inset dM/dH curve, shows one sharp peak at the coercivity field, indicating the magnetization reversal is completed in one-step. The 50 nm unbiased ring, [Fig. 2(c)], clearly shows a constricted shape with a two-step transition during magnetization reversal and zero remanence magnetization, which is typical for the vortex state. The corresponding dM/dH plot shows two well separated peaks. The first switching field $H_{c1} = 96$ Oe, corresponds to the switching from the positive saturated state to the vortex state. The second switching field $H_{c2} = -262$ Oe, corresponds to the switching from vortex state to the reversed saturated state in the negative direction. In between these two switching steps, the vortex state is stable from -28 to -152 Oe. The representative behavior between these two limiting cases of 10 nm and 50 nm is shown for the 30 nm unbiased ring in Fig. 2(b). The dM/dH curve of the descending branch shows two distinct peaks, yet these two peaks are partially overlapping, which indicates that the second reversal step is initiated before the completion of the first step, without a stable vortex state formed in between. Thus, for the unbiased ring, as the thickness of the Fe layer increases from 10 to 50 nm, the hysteresis loop evolves from single-step to double-step, with the transition taking place somewhere between 10 to 30 nm.

For exchange biased rings [Figs. 2(d)–2(f)], the ultra thin 10 nm sample [Fig. 2(d)] also shows a single step transition with a slightly higher coercivity (H_c =130 Oe) and a shift of the loop in the field cool direction $H_{eb} = -81$ Oe, due to the interfacial exchange coupling between Fe and IrMn layer. As the thickness of the Fe layer, t_{Fe}, increases to 50 nm, the hysteresis loop shows a tilted shape with a wide one-step transition centered at -130 Oe, the shift of the loop H_{eb} has decreased to $H_{eb} = -15.2$ Oe. Further increase of the thickness of the Fe layer to 80 nm, causes the shift of the loop to become too small to be detected and the hysteresis evolves into a double-step loop. Thus, compared to the unbiased sample, the hysteresis loops of the exchange biased ring also shows a single-step to double-step transition as t_{Fe} increases, but the transition thickness is shifted higher between 50 nm to 80 nm.

The increase of transition thickness in EB samples could be interpreted by analyzing the magnetic anisotropy induced by the exchange bias on the ring structure. The induced magnetic anisotropy, which consists of a unidirectional component H_E and a collinear uniaxial component H_U,[19,20] is studied by measuring the angular dependence of the exchange bias field H_{eb} and then numerically fitted with an improved effective field model.[19] In the measurements, the magnetic field is applied at an angle α, varying from 0° to 360°, at a step size of 10°, with respective to the bias direction ($\alpha = 0°$). The exchange bias field H_{eb} is obtained at each α value and organized and shown in Fig. 3(a). As shown in this figure, in EB ring samples, the exchange bias field $H_{eb}(\alpha)$ shows a unidirectional symmetry about the bias direction, i.e., $H_{eb}(\pi + \alpha) = -H_{eb}(\alpha)$, and shows a maximum value away from the exchange bias axis ($\alpha = 0°$), due to the existence of the collinear uniaxial anisotropy H_U.[19] To reveal the magnitude of the unidirectional anisotropy H_E and uniaxial anisotropy H_U, the angular dependence of the exchange bias field H_{eb} was numerically fitted with an improved effective field model.[19,20]

For our polycrystalline EB ring sample, the energy per unit volume of the system is given by

$$E = -M_s H \cos(\theta - \alpha) - K_E \cos\theta - K_U \cos^2\theta, \qquad (1)$$

where M_S is the saturation magnetization, H is the applied field. θ and α are the angles between the anisotropy direction

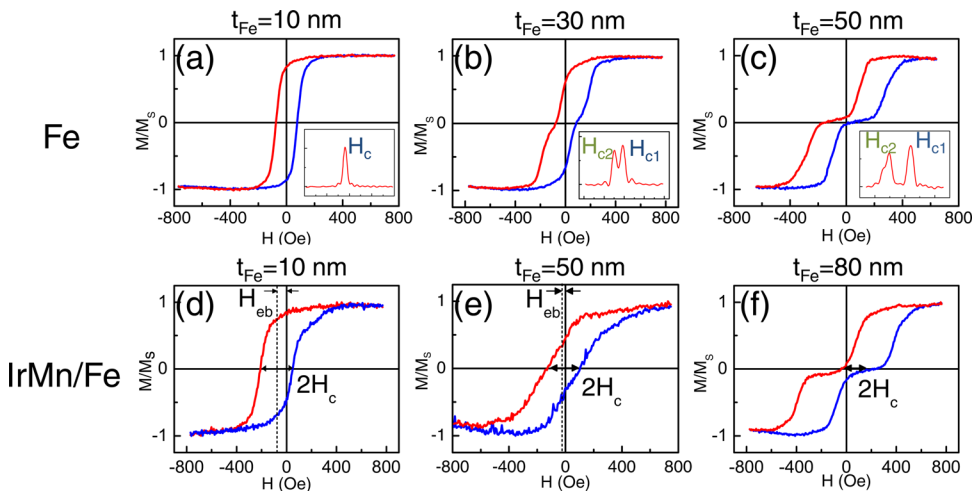

FIG. 2. (Color online) M-H hysteresis loops of unbiased Fe ring arrays with Fe layer thickness equals to (a) 10 nm, (b) 30 nm, and (c) 50 nm. The first order derivative dM/dH of the loop's descending branch is plotted in the inset box located at the right bottom corner of each loop. Hysteresis loops of exchange biased IrMn/Fe rings with t_{Fe} equals to (d) 10 nm, (e) 50 nm, and (c) 80 nm are shown in the second row.

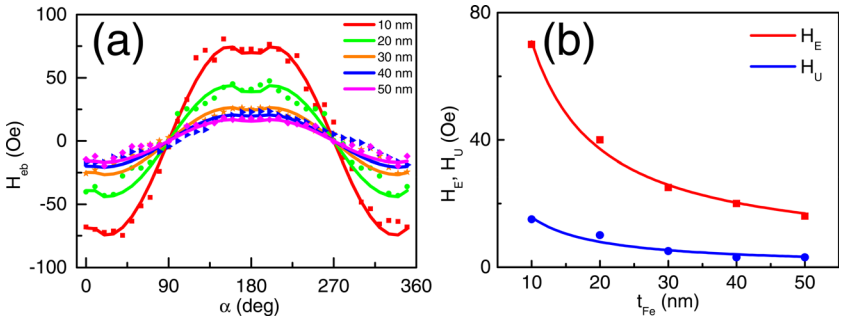

FIG. 3. (Color online) (a) Experimental exchange biased field (symbols) as a function of the field orientation θ and the numerical fitting (continuous line). (b) The anisotropy fields H_{eb} and H_U obtained from the fitting for the angular dependence of H_{eb} for EB IrMn/Fe rings with different t_{Fe}.

and the magnetization and the applied field direction, respectively. The parameters K_E and K_U are determined by $K_E = H_E M_S$ and $K_U = (1/2)H_U M_U$, where H_E and H_U are the effective unidirectional and uniaxial anisotropy field.

To obtain the equilibrium position of the magnetization, we let $\partial E/\partial\theta = 0$ and $\partial^2 E/\partial\theta^2 > 0$, which gives us

$$M_S H \sin(\theta - \alpha) + K_E \sin\theta + K_U \sin 2\theta = 0, \quad (2)$$

$$M_S H \cos(\theta - \alpha) + K_E \cos\theta + 2K_U \cos 2\theta > 0. \quad (3)$$

Solve Eq. (2) for H, we get

$$H(\theta) = \frac{K_E \sin\theta + K_U \sin 2\theta}{\sin(\alpha - \theta)}. \quad (4)$$

The hysteresis loop for a measuring at a specific α value is thus obtained by plot $H(\theta) \sim M_S \cos(\alpha - \theta)$. By letting α varying from 0 to 360 deg, we are able to calculate the angular dependence behavior of the exchange bias field H_{eb} for a given (K_E, K_U)value and compare it with the measured $H_{eb}(\alpha)$ data. The results of the numerical fittings of the effective anisotropy fields are shown in Fig. 3(b).

As shown in Fig. 3(b), the fitted values of the effective unidirectional anisotropy field, H_E and the collinear effective uniaxial anisotropy field, H_U both decreases inversely with the Fe layer thickness, following the $1/t_{Fe}$ dependence.

The effective unidirectional anisotropy field H_E causes the hysteresis loop of the EB sample to shift in the field direction, while the effective uniaxial anisotropy field H_U changes the shape of the hysteresis loop in the EB ring samples. In unbiased Fe rings, the major difference for the single-step switching and double-step switching in ring structure is the remanence state. While in typical single-step switching, the ring remains a quasi-uniform state at remanence, in double-step switching process, the ring forms a vortex remanence state. In EB rings, the uniaxial anisotropy induced by the exchange bias increases the energy density of forming the vortex state by 1/2 K_U,[21,22] while the energy density of the quasi-uniform state stays the same (because spins are aligned with the easy axis). Thus, compared to unbiased Fe rings, EB rings with the induced uniaxial anisotropy prefer single-step switching over double-step switching during reversal. However, as the thickness of the Fe layer increase, the strength of the uniaxial anisotropy will decreases and become negligible [Fig. 3(b)], and then the thick EB ring will show double-step switching again, as we observed in Figs. 2(d)–2(f).

In summary, we systematically studied the effect of exchange bias (EB) on the magnetization reversal behavior in lithographic IrMn/Fe rings and their unbiased Fe counterparts, with the thickness of the Fe layer, t_{Fe}, varying from 10 to 80 nm. It is shown that, as t_{Fe} increases, the hysteresis loops of both unbiased and biased ring undergoes a transition from single-step to double-step. However, for EB samples, this transition happens at larger thickness, which is attributed to the uniaxial anisotropy induced by exchange bias in the Fe layer. The magnitude of this uniaxial anisotropy is studied by measuring the angular dependence of the exchange bias field and fitted numerically with an improved effective model.

The authors would like to thank Wei Zhang for the technical help on the photolithography and Dr. M. Sheinfein for help on micromagnetic simulations. This work was supported by DoE/BES under Grant No. ER45987.

[1]A. O. Adeyeye and N. Singh, J. Phys. D: Appl. Phys. **41**, 153001 (2008).
[2]M. Kläui, C. A. F. Vaz, L. J. Heyderman, U. Rudiger, and J. A. C. Bland, J. Magn. Magn. Mater. **290**, 61 (2005).
[3]C. A. F. Vaz, M. Kläui, L. J. Heyderman, C. David, F. Nolting, and J. A. C. Bland, Phys. Rev. B **72**, 224426 (2005).
[4]S. P. Li, D. Peyrade, M. Natali, A. Lebib, Y. Chen, U. Ebels, L. D. Buda, and K. Ounadjela, Phys. Rev. Lett. **86**, 1102 (2001).
[5]J. Rothman, M. Kläui, L. Lopez-Diaz, C. A. F. Vaz, A. Bleloch, J. A. C. Bland, Z. Cui, and R. Speaks, Phys. Rev. Lett. **86**, 1098 (2001).
[6]J. Zhu, Y. Zheng, and G. A. Prinz, J. Appl. Phys. **87**, 6668 (2000).
[7]J. L. Landro, T. J. Hayward, D. Morecroft, J. A. C. Bland, F. J. Castaño, I. A. Colin, and C. A. Ross, Appl. Phys. Lett. **91**, 203904 (2007).
[8]M. Kläui, C. A. F. Vaz, J. A. C. Bland, W. Wernsdorfer, G. Faini, E. Cambril, L. J. Heyderman, F. Nolting, and U. Rudiger, Phys. Rev. Lett. **94**, 106601 (2005).
[9]E. Saitoh, M. Kawabata, K. Harii, H. Miyajima, and T. Yamaoka, J. Appl. Phys. **95**, 1986 (2004).
[10]X. S. Gao, A. O. Adeyeye, and C. A. Ross, J. Appl. Phys. **103**, 063906 (2008).
[11]J. Nogués, J. Sort, V. Langlais, S. Suriñach, V. Skumryev, J. S. Muñoz, and M. D. Baró, Phys. Rep. **422**, 65 (2005).
[12]Z. B. Guo, Y. K. Zheng, K. B. Li, Z. Y. Liu, P. Luo, and Y. H. Wu, J. Appl. Phys. **95**, 4918 (2004).
[13]W. Jung, F. J. Castano, and C. A. Ross, Phys. Rev. Lett. **97**, 247209 (2006).
[14]W. Jung, F. J. Castano, D. Morecroft, C. A. Ross, R. Menon, and H. I. Smith, J. Appl. Phys. **97**, 10113 (2005).
[15]Y. Hou, Q. Zhan, and K. M. Krishnan, Appl. Phys. Lett. **98**, 042510 (2011).
[16]D. Tripathy, A. O. Adeyeye, N. Singh, and R. L. Stamps, Nanotechnology **20**, 015304 (2009).
[17]W. Zhang, D. N. Weiss, and K. M. Krishnan, J. Micromech. Microeng. **21**, 045024 (2011).
[18]H. S. Jung, H. Fujiwara, and S. Matsunuma, J. Magn. Magn. Mater. **286**, 229 (2005).
[19]J. Camarero, J. Sort, A. Hoffmann,J. M. Garcia-Martin, B. Dieny, R. Miranda, and J. Nogues, Phys. Rev. Lett. **95**, 057204 (2005).
[20]Q. Zhan and K. M. Krishnan, J. Appl. Phys. **107**, 09D703 (2009).
[21]H. Hoffmann and F. Steinbauer, J. Appl. Phys. **92**, 9 (2002).
[22]S. P. Li, W. S. Lew, and J. A. C. Bland, M. Natali, A. Lebib, and Y. Chen, J. Appl. Phys. **92**, 7397 (2002).